Beam dynamics for cyclotrons

F. Chautard
Grand Accélérateur d'Ions Lourds (GANIL), Caen, France

Abstract
This paper intends to introduce the beam dynamics in the cyclotron. The long history of the cyclotron evolution is reminded and the different developments since 1929 from E. Lawrence's great idea are reviewed from conventional cyclotron to synchrocyclotron. The transverse and longitudinal beam dynamics are detailed as well as the specific quantities applied to cyclotron. Finally, and since the study of the dynamics in cyclotrons differs from the one in synchrotrons due to the non-periodic lattice, an opening to beam dynamics computation is proposed to handle the peculiar way of cyclotron tuning. A list of books, articles and proceedings is referred to the end to go deeper in the subject

1 Introduction

The need from nuclear physicists to get ions with higher and higher kinetic energies, obliged engineers to design accelerating structures. In 1932, Cockroft and Walton, from Cambridge, built an accelerator capable of developing an accelerating voltage up to 700 000 volts for the acceleration of protons.

Simultaneously, Robert van De Graaf reached 1.5 MV D.C. with a machine afterwards named after him. But, electrostatic machines are very sensitive machines, due mainly to breakdowns. Then, in 1928, Rolf Wideröe, imagined, a linear accelerator bringing Sodium and Potassium ions up to 50 keV. The beam needs to pass a large number of drift tubes to be accelerated. In 1929, Ernest Lawrence, from Berkeley, inspired by an article by Wideröe, had the idea to put the beam and the cavity inside one, large dipole in order to curve the particle trajectory and have only one accelerating cavity [1].

Figure 1 shows schematically the evolution from a linear accelerator to a cyclotron. Figure 2 illustrates the first accelerating cavities (called Dees). One cavity is at ground and the opposite at an other alternating potential.

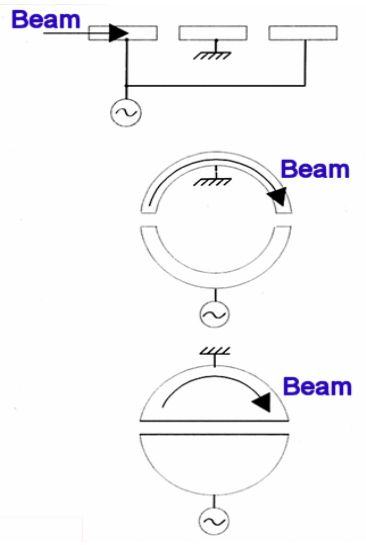

Fig. 1: From a linear structure to the cyclotron

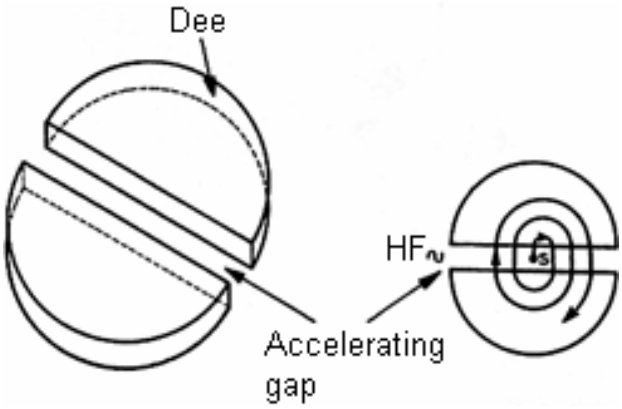

Fig. 2: First accelerating cavities in cyclotron called Dees

2 Conventional cyclotron

"Conventional" means here a cyclotron operating with a uniform magnetic field generated by a magnet with flat parallel pole tips. It was the first cyclotron ever designed. Let us consider an ion with a charge q and a mass m circulating at a speed v_θ in a uniform induction field B. The motion equation can be derived from the Lorentz force F and the Newton's law

$$\vec{F} = q(\vec{v} \times \vec{B}) \tag{1}$$

$$\frac{d(m\vec{v})}{dt} = \vec{F} \tag{2}$$

for obvious practical reasons, cylindrical coordinates are used . (1) and (2) become

$$\frac{d(m\dot{r})}{dt} - mr\dot{\theta}^2 = q[r\dot{\theta}B_z - \dot{z}B_\theta] \tag{3}$$

$$\frac{d(mr\dot{\theta})}{dt} + m\dot{r}\dot{\theta} = q[\dot{z}B_r - \dot{r}B_z] \tag{4}$$

$$\frac{d(m\dot{z})}{dt} = q[\dot{r}B_\theta - r\dot{\theta}B_r] \tag{5}$$

where dotted symbols are the derivatives with respect to time. Since the energy gained in this first type of cyclotron is small, we can consider the dynamics for a non-relativistic particle ($\gamma \sim 1$) where $m = m_0$. Taking the magnetic field B_z along the negative z-axis: $B_z = -B_0$, the equations become

$$m_0(\ddot{r} - r\dot{\theta}^2) = -qr\dot{\theta}B_0 \tag{6}$$

$$m_0(r\ddot{\theta} + 2\dot{r}\dot{\theta}) = q\dot{r}B_0 \tag{7}$$

$$m_0\ddot{z} = 0 \tag{8}$$

with the beam initial conditions $(\dot{r} = 0,\ \dot{\theta},\ \dot{z} = 0)$, the equations (6), (7) and (8), the trajectory is a circle (Fig 3). It is called closed orbit in the median plane (r, θ). The radius is r and the angular velocity (Larmor frequency f_{rev}):

$$\omega_{rev} = \dot{\theta} = \frac{f_{rev}}{2\pi} = \frac{qB_0}{m_0} \tag{9}$$

the magnetic rigidity is defined by

$$B_0 r = \frac{p}{q} \tag{10}$$

with $p = m_0 v$ the particle momentum. During acceleration and in this non-relativistic domain ($\gamma \sim 1$), the revolution frequency ω_{rev} remains constant. The particle takes the same time to make one turn which defines the **isochronism condition**.

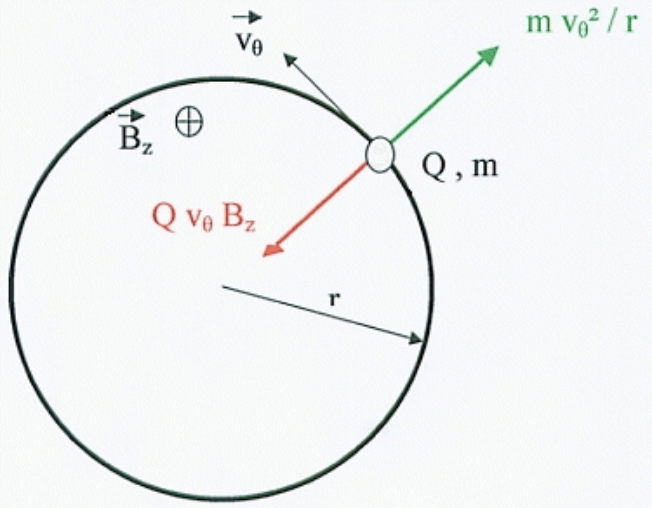

Fig. 3: Field and forces layout on a closed orbit for a classic cyclotron

The applied RF accelerating voltage between the Dees

$$V = V_0 \cos(\omega_{RF} t) \tag{11}$$

the synchronism condition is

$$\omega_{RF} = h\omega_{rev} \tag{12}$$

where h = 1, 2, 3 ... is called the RF harmonic mode. It is obvious now that the beam is bunched with the same time structure than the RF field, each bunch laying on an accelerating wave. Figure 4 shows the bunch position with respect to the RF accelerating wave at each gap crossing between the two Dees. With this simple configuration and with the isochronous and synchronous conditions between the particle, the RF field and magnetic field, the beam arrives always at the same optimum accelerating RF phase. The AC generator alternates the polarity of the Dees in order to give to the ion an accelerating field every half period. With 180° Dees, if the harmonic number is 1, only one beam can be accelerated per turn.

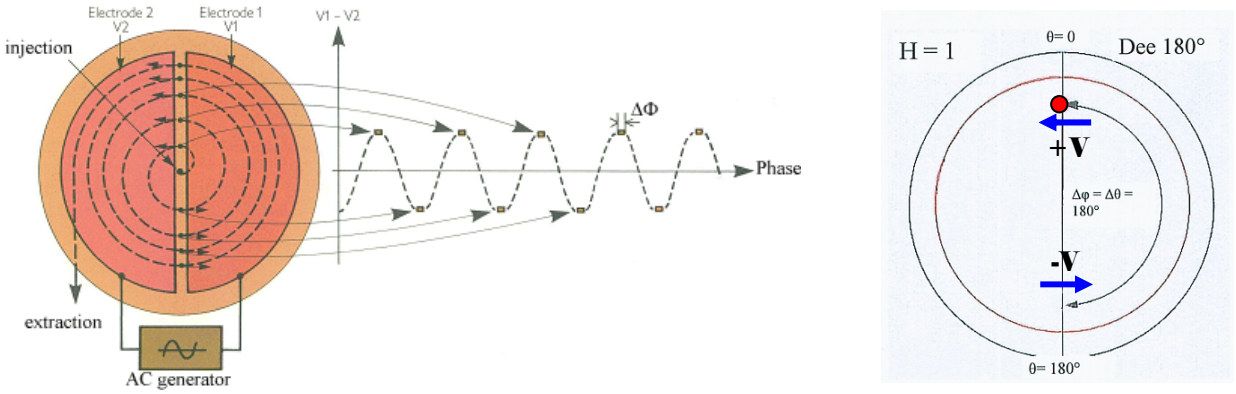

Fig. 4: Accelerating field configuration with Dees on harmonic 1

The kinetic energy of the beam out of the cyclotron at a radius r will be

$$W = \frac{1}{2} m_0 v^2 = \frac{1}{2} m_0 (2\pi r f_{rev})^2 = \frac{1}{2} m_0 (2\pi r \frac{f_{rf}}{h})^2 \quad .$$

The frequency dependence is one of the limiting factor for the acceleration. A fixed frequency range available from the AC generator, given by the technology constraints, gives a fixed range of kinetic energy (depending on f_{rf}^2 with $h = 1$). But, the energy range can be extended through the harmonic number. With the same magnetic and cavity configuration, the next possible harmonic is $h = 3$ (Fig. 5), the beam velocity is 3 times smaller and there are 3 bunches per turn. Lower energies are reachable.

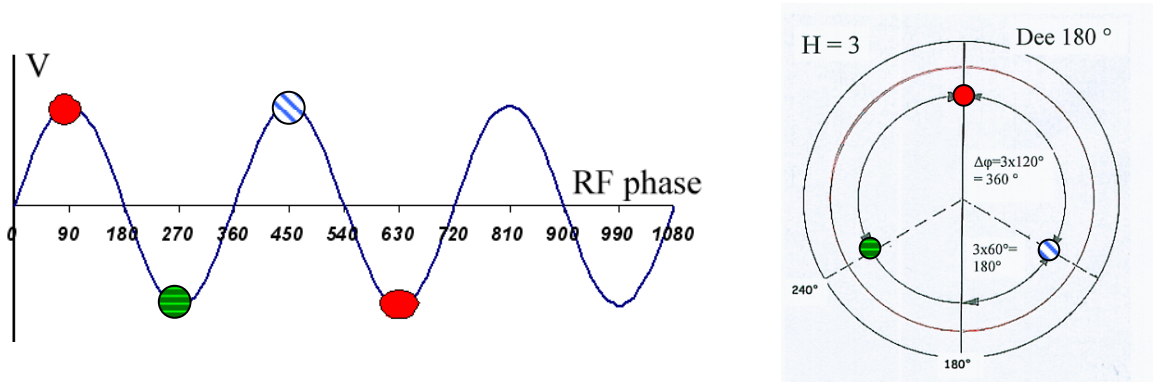

Fig. 5: Other acceleration configuration with $h = 3$

2.1 Transverse dynamics

2.1.1 Horizontal stability

The cylindrical coordinates *(r, θ, z)* are well suited to express the particle motion in a cyclotron. Figure 6 recalls the coordinate system. For the ideal reference particle, we define a closed orbit with a radius ρ and consider the motion of particles with small orbit deviations (paraxial condition) around this trajectory such as:

$$r = \rho + x = \rho(1 + \frac{x}{\rho})$$

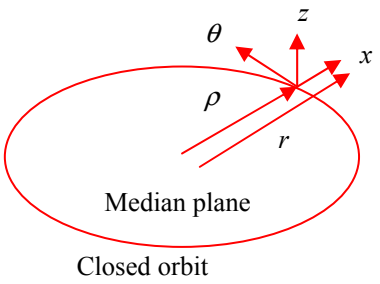

Fig. 6: Coordinates system attached to the reference particle on the closed orbit

The magnetic field (0, 0, B_z) around the median plane is expanded in Taylor series along the radial dimension

$$B_z = B_{0z} + \frac{\partial B_z}{\partial x} x = B_{0z}\left(1 + \frac{\rho}{B_{0z}} \frac{\partial B_z}{\partial x} \frac{x}{\rho}\right) = B_{0z}\left(1 - n \frac{x}{\rho}\right) \tag{13}$$

and we define the field index as the fractional change of the axial component of the field $B_z(x)$ associated with a fractional change of radius (can be expressed also as $n = -k$)

$$n = -\frac{\rho}{B_{0z}} \frac{\partial B_z}{\partial x} \tag{14}$$

Particles on the closed orbit see the centrifugal force compensating the horizontal restoring force

$$\frac{m v_\theta^2}{r} = q v_\theta B_z \tag{15}$$

For particles off the closed orbit, a restoring force F_x appears

$$F_x = \frac{m v_\theta^2}{r} - q v_\theta B_z \tag{16}$$

inserting (13) into (16)

$$F_x = \frac{m v_\theta^2}{\rho}\left(1 - \frac{x}{\rho}\right) - q v_\theta B_{0z}\left(1 - n \frac{x}{\rho}\right) = -\frac{m v_\theta^2}{\rho} \frac{x}{\rho}(1 - n) \tag{17}$$

Recalling Newton's law $F_x = m\ddot{x}$, we finally find

$$\ddot{x} + \frac{v_\theta^2}{\rho^2}(1 - n)x = 0 \tag{18}$$

$$\ddot{x} + \omega_r^2 x = 0 \tag{19}$$

which is the equation of an harmonic oscillator with $\omega_r = \sqrt{1-n}\ \omega_0$ and $\omega_0 = v_\theta/\rho$ the angular velocity of the particle on the closed orbit and the horizontal betatron number $\nu_r = \sqrt{1-n}$ (ν_r can be called Q_r in the literature). The motion is stable only if $n < 1$

A selected particular solution in the median plane is

$$x(t) = x_{max} \cos(\nu_r \omega_0 t) \tag{20}$$

As an example, Fig 7, the particle makes nine horizontal oscillations for 10 turns in the cyclotron which is directly related to the betatron number $\nu_r = 9/10 = 0{,}9$

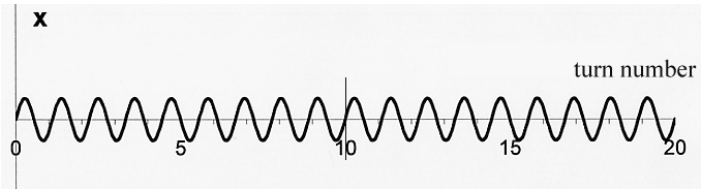

Fig. 7: Horizontal betatron oscillations

2.1.2 Vertical stability

Similarly, in the vertical plane we have a restoring force F_z such as

$$F_z = m\ddot{z} = q\ v_\theta B_x \tag{21}$$

Because $\nabla \times B = 0$, $\frac{\partial B_x}{\partial z} - \frac{\partial B_z}{\partial x} = 0$, we get $B_x = -n\frac{B_{0z}}{\rho} z$. By substitution in (21), the vertical equation of motion is

$$\ddot{z} + \omega_z^2 z = 0 \tag{22}$$

which is the equation of a harmonic oscillator with $\omega_z = \sqrt{n}\ \omega_0$ and the vertical betatron number is $\nu_z = \sqrt{n}$. The motion is stable only if $n > 0$

The oscillations around the median plane are described by

$$z(t) = z_{max} \cos(\nu_z \omega_0 t) \tag{23}$$

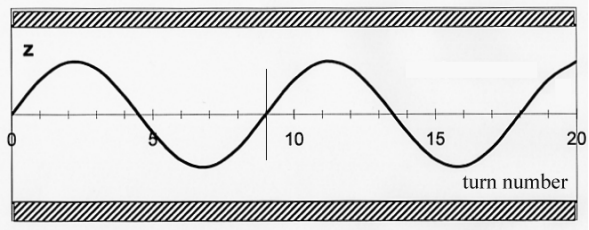

Fig. 8: Vertical betatron oscillation

In Fig 8, one vertical oscillation for 9 turns in the cyclotron gives $\nu_z = 1/9 = 0{,}11$

2.1.3 Weak focusing

During acceleration, simultaneous horizontal and vertical stability are needed, therefore, the field index *n* should be bounded between 0 and 1 (*weak focusing definition*) which is, by the definition of *n*, the characteristic of a slightly decreasing field.

Equation (9) shows the dependence of the revolution frequency on the magnetic field. If the magnetic field decreases, ω_{rev} will also decrease. Then a phase difference $\Delta\phi$ between the accelerating field phase and the beam will build up such as:

$$\Delta\varphi = \pi \cdot \left[\left(\omega_{RF} / \omega_{rev} \right) - 1 \right].$$

The synchronism condition (12) is fulfilled only at one radius for the so-called *isochronous bunch* (Fig. 9).

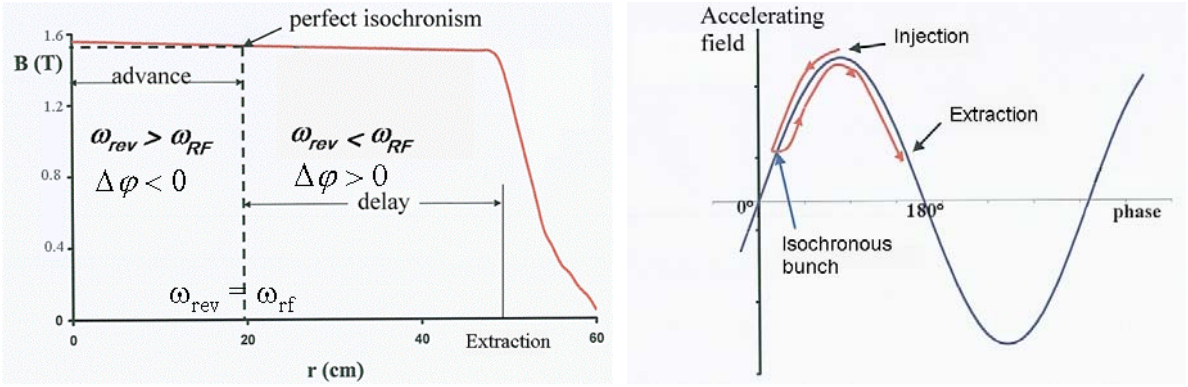

Fig. 9: Beam phase evolution in a conventional flat pole cyclotron

The focusing condition is not compatible with the isochronism of the machine. The beam extraction should be done before reaching the decelerating phase region. The energy range is limited by the geometry of the cyclotron. The weak focusing does not allow to get high energies.

3 Azimuthally Varying Field (AVF) cyclotron

When higher energies are aimed at, the relativistic mass increase during the acceleration cannot be neglected anymore and $m = \gamma m_0$ should be put in the previous equations. The revolution frequency ω_{rev} is then dependent on $1/\gamma$ [Eq. (9)].The isochronism condition can only be fulfilled if the mean field increases as γ.

$$\bar{B}_z(r) = \gamma(r)\bar{B}_z(0) \tag{24}$$

This is clearly in opposition to the weak focusing condition and a vertical focusing. In 1938, Thomas discovered that to improve the vertical focusing, sectors have to be inserted [2] and [3]. The succession of hills and valleys creates an azimuthal field modulation (Fig. 10 and Fig. 11). A B_θ component of the field appears and as the trajectory of the beam is no longer a circle, a component v_r of the beam speed is created. Therefore, the vertical component $F_z \propto v_r \,.\, B_\theta$ of the Lorentz force is created.

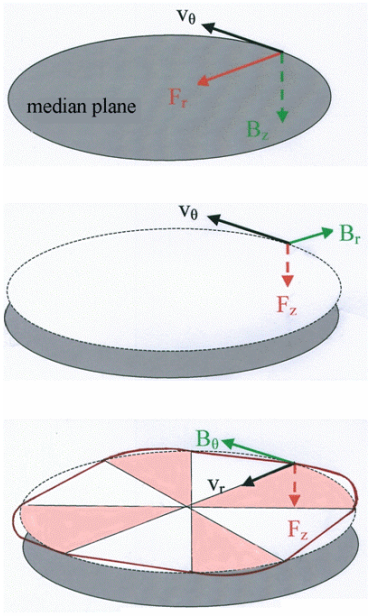

Fig. 10: Creation of a new vertical force to compensate the field increase necessary to the isochronism condition

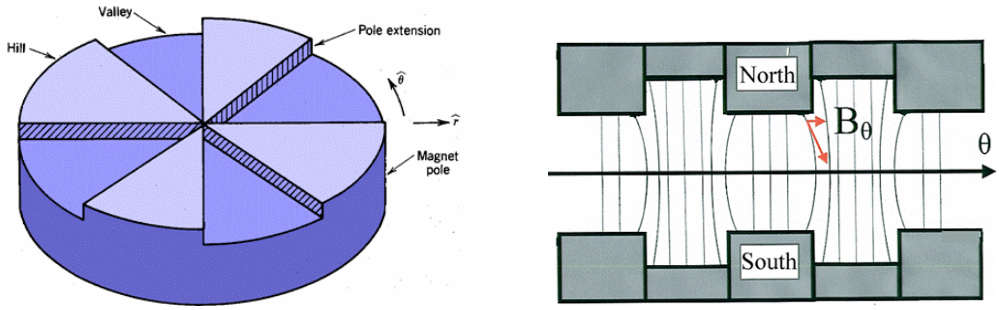

Fig. 11: Sectors to create azimuthal field modulation

The field modulation induced by the sectors can be express through the flutter F defined by:

$$F_l = \frac{\langle B^2 \rangle - \langle B \rangle^2}{\langle B \rangle^2} \approx \frac{\left(B_{\text{hill}} - B_{\text{val}}\right)^2}{8\langle B \rangle^2} \tag{25}$$

where $\langle B \rangle$ is the field average over one turn. To ease the comprehension, the flutter term can also be expressed into hill and valley terms.

From (21) and (22), the vertical focusing force strength $|F_z| = \omega^2 z = v_z^2 \cdot \omega_0^2 z \approx v_z^2$

For a cyclotron with N sectors, the betatron number depends on the flutter term such as

$$F_z \approx v_z^2 = n + \frac{N^2}{N^2 - 1} F_l + \ldots \tag{26}$$

Therefore, the flutter term F_l enhances the initial weak focusing term n.

With (14) and (24) and for high energies, γ^2 is greater than 1

$$n = -\frac{r}{\gamma}\frac{d\gamma}{dr} = 1 - \gamma^2 < 0 \tag{27}$$

the field index becomes negative and the particle motion is unstable. To reach high beam energy (γ^2 term), and a stable motion $\nu_z > 0$, the condition on the flutter term is the following

$$\frac{N^2}{N^2 - 1} F_l > -n = \gamma^2 - 1 \tag{28}$$

Remark: Increasing the number of sector does not help in the focusing [$N^2/(N^2-1)$ term slightly decreases with N]. The choice to increase the number of sector N derives from resonance considerations developed in §8.4

Then, we find that to aim at high energies where the Lorentz factor becomes large one has to increase the flutter term to keep an efficient vertical focusing effective, which is possible from (25) by lowering the field in the valley down to zero leading to the separated sector cyclotron

4 Spiral sector cyclotron

In 1954, Kertz realised that spiralling sectors by an angle ξ, the valley-hill transition became more focusing while the hill-valley transition was less focusing. But by the strong focusing principle (larger betatron amplitude in focusing, small in defocusing), the net effect is focusing.

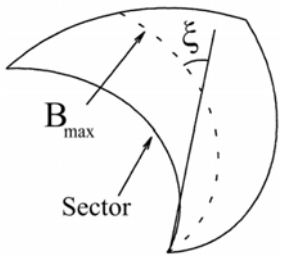

Then an additional term is added to the vertical restoring force

$$F_z \approx \nu_z^2 = n + \frac{N^2}{N^2 - 1} F_l (1 + 2\tan^2 \xi) \ . \tag{29}$$

Similarly, in the radial plane

$$F_r \approx \nu_z^2 = 1 - n + \frac{3N^2}{(N^2 - 1)\cdot(N^2 - 4)} F_l (1 + 2\tan^2 \xi) \ . \tag{30}$$

5 Superconducting cyclotron

Most of the cyclotrons utilize room temperature magnets with a maximum induction field of 2 Tesla coming from the iron saturation. Beyond this limit, superconducting coils are used and 6 Tesla can be reached. The magnets are smaller and this technology lowers also the operational cost. The maximum energy per nucleon capability of a cyclotron is given by

$$W = \frac{(B\rho)^2 e^2}{2m_u}\left(\frac{Q}{A}\right)^2 = K_b\left(\frac{Q}{A}\right)^2 \tag{31}$$

where A is the number of nucleon, K_b is the so-called bending factor of the cyclotron, m_u is the atomic mass unit, e the charge unit and, $q = Qe$. But for superconducting cyclotrons, the iron is saturated, the term $(B_{hill} - B_{val})^2$ is constant and $F_l \approx 1/\langle B \rangle^2$. The consequence is that for high energy per nucleon requiring high magnetic fields, the superconducting cyclotrons see their vertical focusing term decrease (Fig. 12).

$$W = K_f \left(\frac{Q}{A} \right) \tag{32}$$

where K_f is the so-called focusing factor of a superconducting cyclotron. If the field is decreased, the focusing limit is increased, the dot-dash line is where the bending and focusing limits are equal and up to which the cyclotron is usable [4].

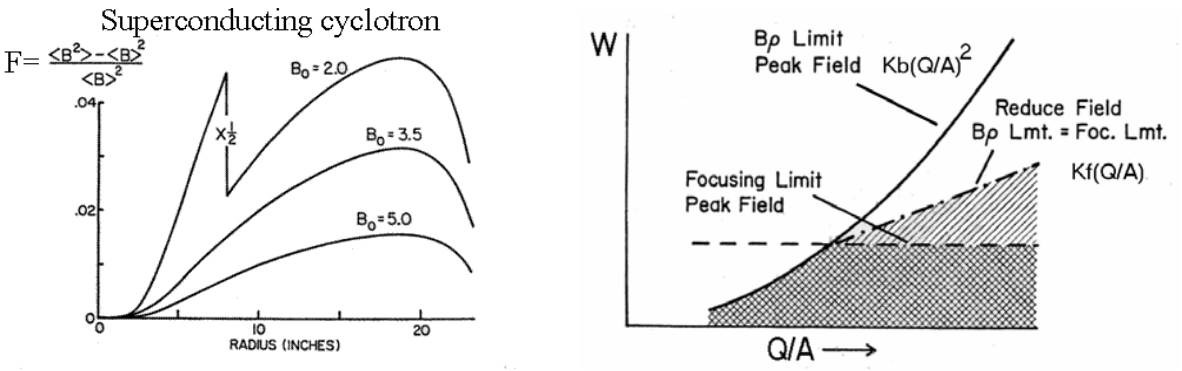

Fig 12: Superconducting cyclotron behaviour and focusing limitation

6 Frequency modulated cyclotron or synchrocyclotron

The last machine to be described is the synchrocyclotron; only four of them remain around the world. This machine has an uniform magnetic field and a positive field index. Therefore, to make an efficient acceleration, the RF frequency needs to be decreased to compensate for the increase of mass ($\omega_{rev} = QB/\gamma m_0 \approx \omega_{rf}$). This is a cycled machine (compared to continuous beam for cyclotrons) and the beam makes thousand turns mainly due to the low voltage applied. This type of machine delivers very high energy beams from MeV to GeV.

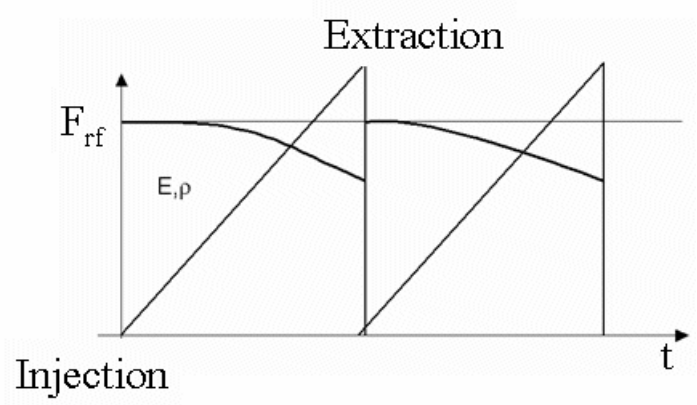

Fig. 13: Synchrocyclotron frequency cycle from the injection to extraction with fixed magnetic field

7 Longitudinal dynamics

A cyclotron can accelerate only a portion of an RF cycle and the acceptance is about ± 20° RF (out of 360°). The external source, such as ECR or EBIS etc. delivers DC-beams compared to the cyclotron RF frequency. A buncher located upstream from the cyclotron injection accelerates particles which would come late to the first accelerating gap and decelerates the ones coming too early. Then, more particles can be accelerated in the cyclotron within the ± 20° acceptance. This increases the cyclotron injection efficiency by a factor 4–6

The final energy is independent of the accelerating potential $V = V_0\cos\varphi$: if V_0 varies, the number of turn varies. The energy gain per nucleon and per turn depends on the peak potential V_0, but is constant, if the cyclotron is isochronous (φ =const): $\delta W = N_g Q/AV_0 \cos\varphi$, where N_g is number of gaps. The radial separation turn between two turns varies as $1/r$ ($\gamma \sim 1$) :

$$\frac{\delta r}{r} = \frac{1}{2}\frac{\delta W}{W} = \frac{Q/AV_0\cos\varphi}{2W} \propto \frac{1}{r^2} \tag{33}$$

7.1 Acceleration with sector cavities (not Dees)

To ease the comprehension, we take the example of the CIME cyclotron at GANIL [5], Caen, France, with two RF cavities whose azimuthal extent are $\alpha = 40°$.The energy gain per turn is $\delta W = Q/AV_0 \sin(h\alpha/2)\cos\varphi$. For a maximum energy gain, the particle crosses the symmetry cavity axis when $\varphi = 0°$ ($\cos\varphi = 1$).

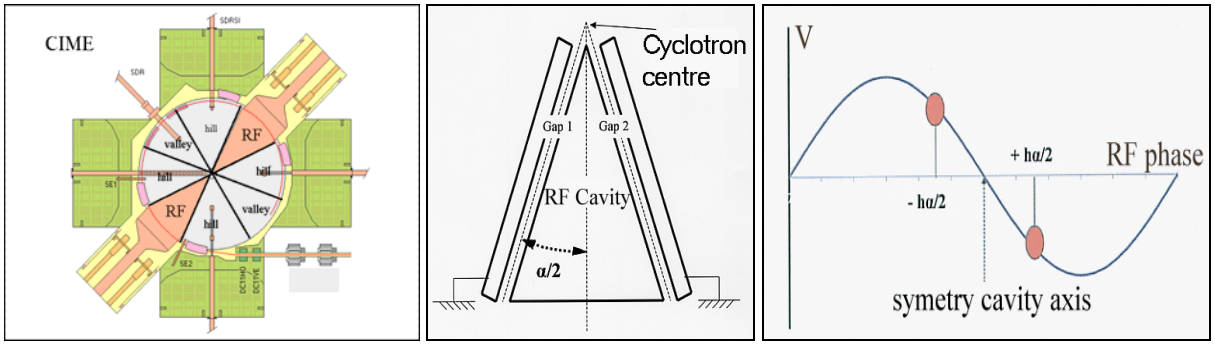

Fig. 14: Acceleration principle with sector cavities

The acceleration is efficient for harmonic numbers up to 8.

h	2	3	4	5	6	7	8
Sin($h\alpha$/2)	0.64	0.87	0.98	0.98	0.86	0.64	0.34

The table below summarizes a few cyclotron characteristics.

Laboratory	Cyclotron name/type	*K* (MeV/n) (or proton energy *Q/A* =1)	Extraction radius (m)
GANIL(FR)	C0	28	0.48
NAC (SA)	SSC	220	4.2
GANIL (FR)	CIME	265	1.5
GANIL (FR)	SSC2	380	3
RIKEN (JP)	RING	540	3.6
PSI (CH)	Ring	592	4.5
DUBNA (RU)	U400	625	1.8
CATANIA(I)	LNS (S.C.)	800 (*kf* = 200)	0.9
MSU (USA)	K1200 (S.C.)	1200 (*kf* = 400)	1

8 Beam dynamics computation

We can assume that along the closed orbit, the particle sees a succession of drift, dipole and focusing lenses. But putting those elements into a transport code is not going to work to fully predict the beam trajectory and envelopes. This is because we do not know *a priori* where the orbit is for any momentum neither the edge angles nor the field index in that region. The only realistic solution is to get the field map from measurements or calculations and compute the equation of motion through it in 2D or 3D [6].

The field map computation by codes is obtained at present with a great accuracy with respect to the measured one (Fig. 15 and Fig. 16) [7]. Since, the field precise configuration varies with the field level, the field maps covering the working diagram (see §10) of the cyclotron has to be determinded. For CIME, 10 levels were necessary. Similarly, the RF field map can be decomposed into two regions: the central region where the beam is injected into the cyclotron and the cavity gaps.

The transport of particles through the 3D field map will predict the behaviour of the beam during the acceleration. One can rely on numerical models even for large machine. The transport of the particle through the accelerating gaps depends on its vertical position. One has to take into account the real equipotential distribution, especially in the central region where the energy is low.

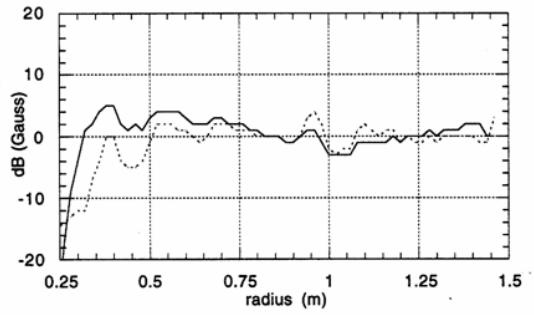

Fig. 15: Comparison between computed/measured magnetic field for CIME

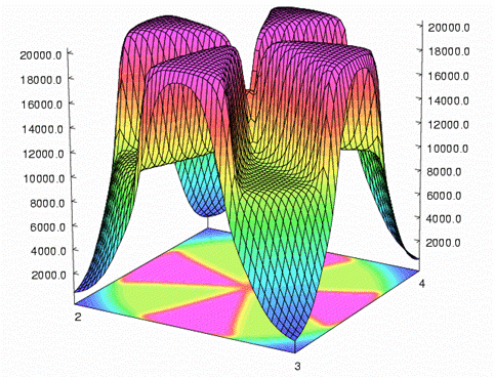

Fig. 16: Field map of CIME with successive high and low field regions (high /valley)

8.1 Trajectories and matching recipes

As the cyclotron cannot be decomposed into periodic lattice, the trajectory is found by an iterative process. To handle the peculiar way of cyclotron tuning here is a short recipes

– Find a reference trajectory (1 particle) for a isochronous field level and a given frequency

find first a closed orbit at large radius with no RF field in the cavities

Then turn on RF field to decelerate the central particle to the injection.

Tune the RF and the magnetic field at the injection to join the injection point out of the inflector.

– Find a matched beam in the cyclotron (multiparticles)

Start with a matched beam at large radius around the central trajectory (see §8.2) without RF field and check the beam matching

Again in backward tracking determine the matched beam (see §8.2, 8.3) at the injection point

– Forward tracking

confirm the matching from the injection to the extraction

fine tune the magnetic field with the isochronism coils

and if the 6D matching at the injection is not completely feasible by the injection line predict the new beam envelope and extraction

– Ejection tracking

Of course this is an iterative process and should be done for the different magnetic field level of the machine.

8.2 Transverse phase space in a cyclotron

The horizontal and vertical beam distributions are described by the emittance areas A_x and A_y assumed to be upright ellipses with axis x_{max}, x'_{max} and z_{max}, z_{max} where x'_{max} and z'_{max} denote the divergence of the particle with respect to the reference particle at the centre of the beam.

As for the FODO cell or in synchrotron, the beam has to be matched to the field configuration in order to minimize the beam envelopes and reduce the effective acceptance. From the equation (18) and (19) at a radius R

$$\begin{cases} x(t) = x_{max}\cos(\nu_r \omega_0 t) \\ x'(t) = \dfrac{dx}{ds} = \dfrac{dx}{R\omega_0 dt} = -(\dfrac{x_{max}\nu_r}{R})\sin(\nu_r \omega_0 t) \end{cases}$$

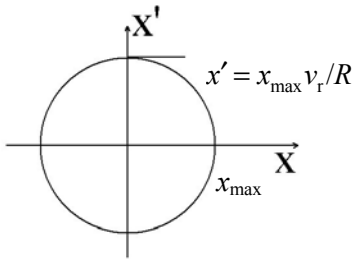

The emittance areas are $A_x = \pi x_{max} \cdot x'_{max} = \pi \cdot x_{max}^2 \nu_r / R$ meaning that all particle included in this surface will remain bounded in it. That initial beam conditions depends on ν_r which varies with the cyclotron field level. If the matching condition $|x'_{max}(t)| = (x_{max}\nu_r/R)\theta$ is not respected, the width of the beam will oscillates with the betatron frequency and the acceptance has to be larger for the same emittance (Fig. 17).

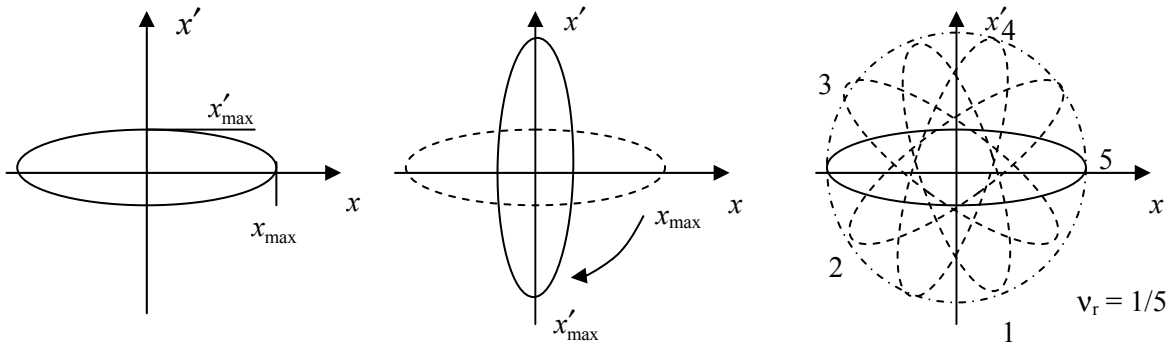

Fig. 17: Radial phase-space evolution for an unmatched beam to the eigenellipse of the cyclotron

A matched beam, Fig. 18, remains matched as long as ν_r and ν_z change slowly under acceleration. Under acceleration and taking into account relativistic mass increase, the normalized emittances ε_x and ε_z remain constant

$$\varepsilon_x = \beta\gamma A_x = \pi\frac{\omega}{c}\gamma x_{max}^2 \nu_r = \text{constant}$$

$$\varepsilon_z = \beta\gamma A_z = \pi\frac{\omega}{c}\gamma z_{max}^2 \nu_z = \text{constant}$$

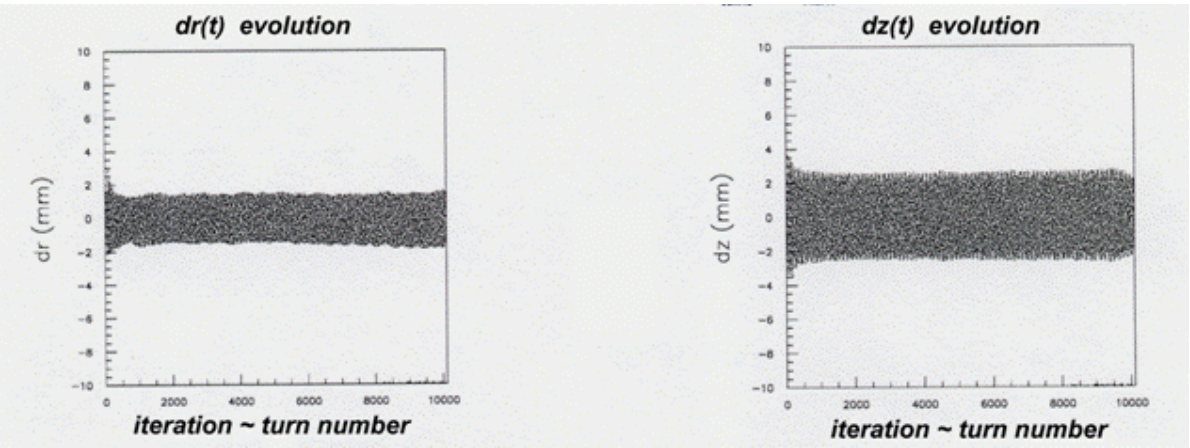

Fig. 18: Radial and vertical matched beam transportation from injection to extraction. $\nu_r \approx 1$ and $\nu_z \approx 0.26$ over the acceleration.

From §2.1.1, the horizontal betatron frequency can be expressed as $\nu_r = \sqrt{1-n} = \gamma$. Since ε_x is constant, x_{max} scales as $1/\gamma$. And because γ does not varies strongly in most cyclotrons, the horizontal dimension x_{max} is considered to remain constant. Therefore, the divergence $\left|x'_{max}(t)\right| = x_{max}\nu_r/R$ varies as $1/R$.

Similarly, the vertical size for a matched beam is proportional to $1/\sqrt{\nu_z\gamma}$ which can be fairly large in the case of weak focusing with ν_z small.

8.3 Backward 6D matching

The determination of the central trajectory and the matched beam at large radius does not allow the determination of the phase space at injection in the cyclotron. A correlation exists within transverse phase space variable and also between transverse and longitudinal phase space. The good matching of the beam in the cyclotron will depend on these initial conditions. As the injection field distribution and acceleration are of great complexity in this region, one solution is to transport a matched beam backward from large radius to this injection point in the cyclotron which can be an inflector or an injection beam line and see how the beam shape evolves.

This refinement in tuning appeared with the external sources. ECR sources, for example, could be placed far from the cyclotron injection and magnetic lenses can be inserted in between, along the transport line, to shape the beam into a matched beam

Figure 19 and Fig. 20 show an example of injection centre and the correlation required for a given field level. A Gaussian distribution is calculated over the particles to determine the representative dimension such as the beam maximum extension and the correlation within the phase space.

Unfortunately, the Gaussian distribution is not always well suited to the particle distribution (see dphi-dpr/p0 plot in Fig 20). One has to check by a forward tracking that the initial mismatch will not be critical. This pattern will be greatly modified as a function of the magnetic field level and harmonic number.

A beam line before the injection point can then create such a predicted correlation with quadrupoles, skew-quadrupoles and/or solenoid for transverse correlation and buncher for the longitudinal dimensions (Fig. 21).

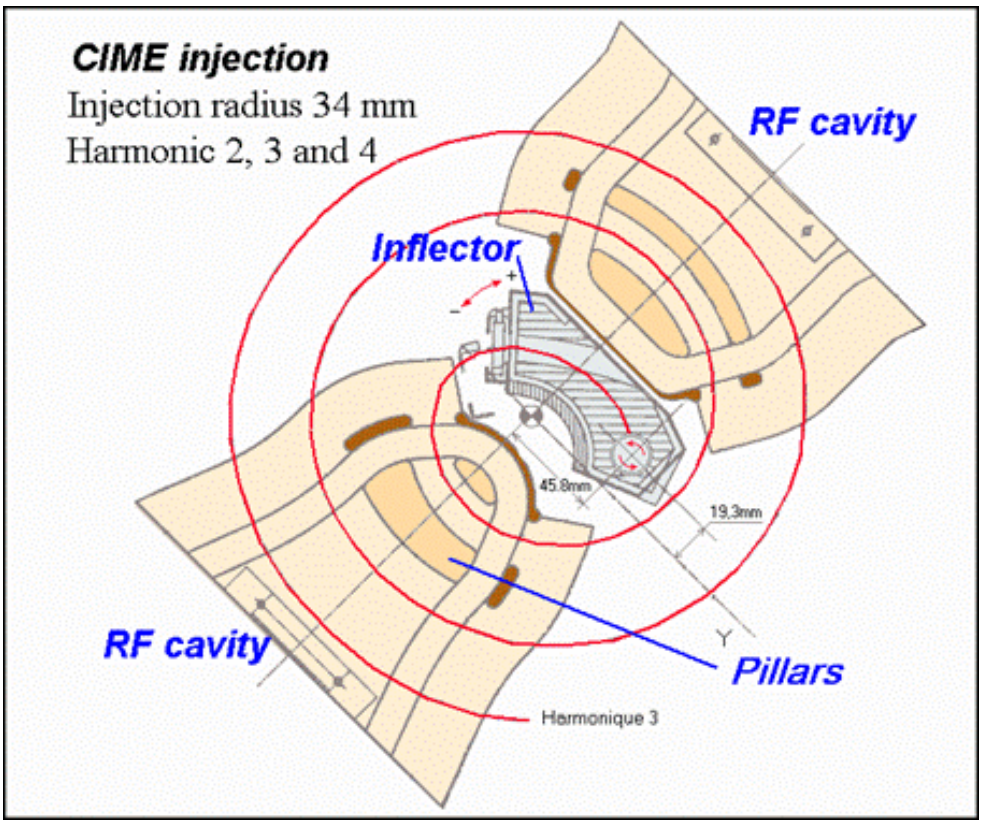

Fig.19: Example of injection centre from the CIME cyclotron with the beam trajectory over the first three turns

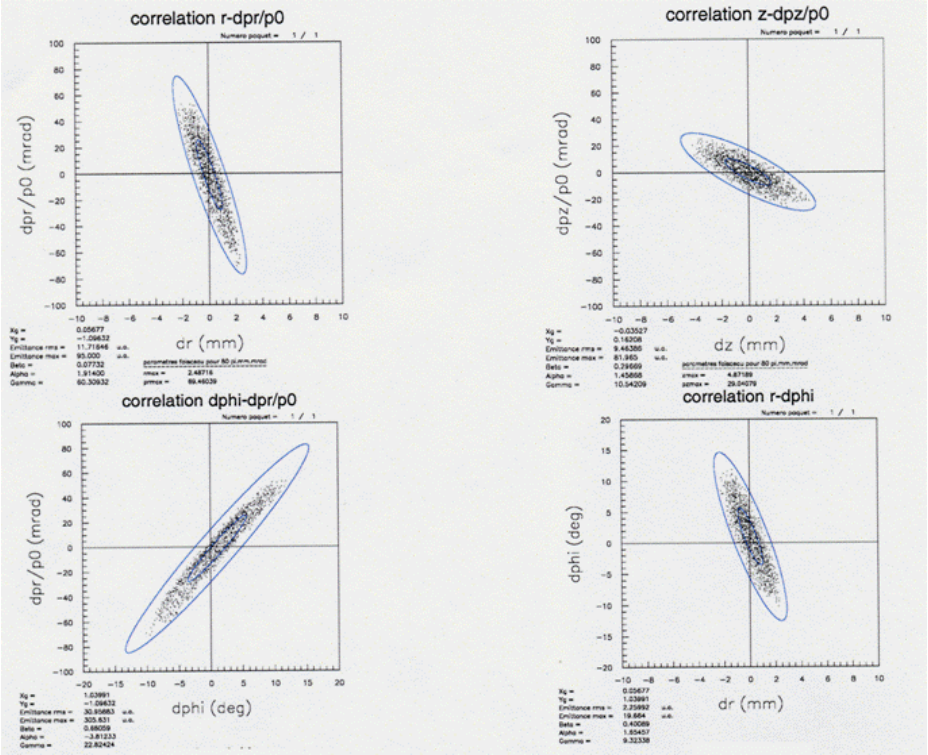

Fig. 20: Phase space out of the inflector in order to get a matched beam during acceleration

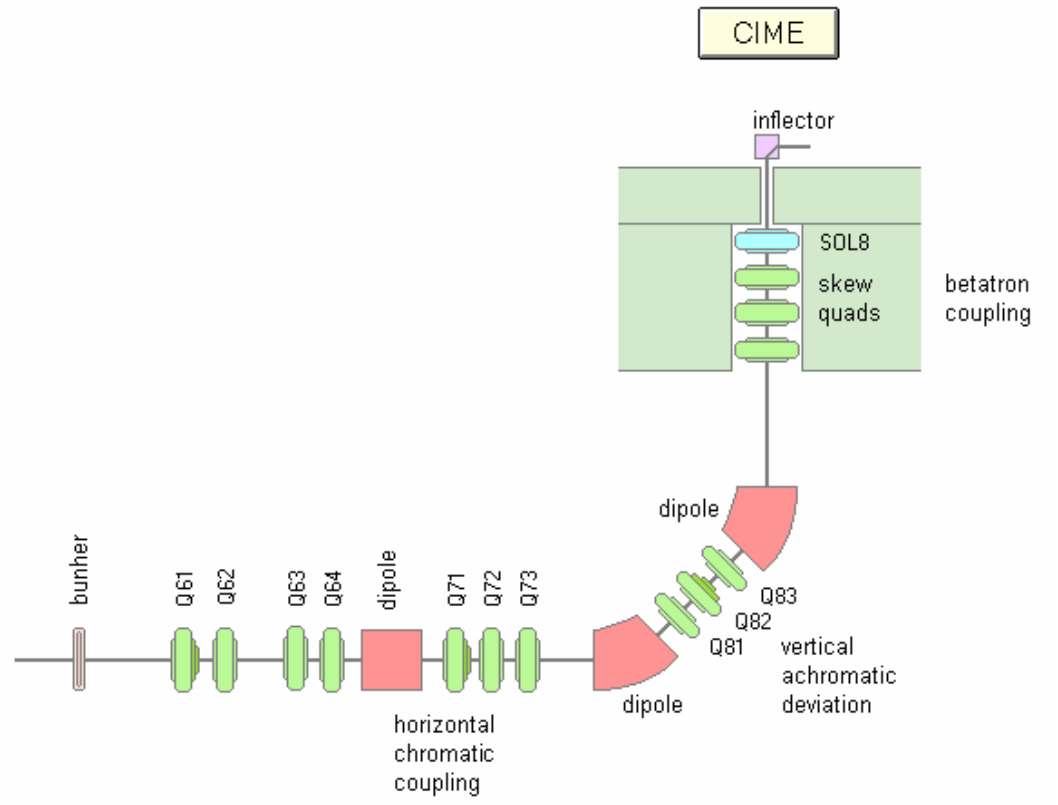

Fig. 21: CIME injection beamline which adapts the beam shape in the 6 D phase-space

8.4 Tunes and resonances

Resonances in an accelerator affect the amplitude of the beam betatron oscillation and may bring the beam to blow out . They are produced by the magnetic field configuration expressed through ν_r and ν_z. Resonances are encountered when

$$K \cdot \nu_r + L \cdot \nu_z = P \tag{34}$$

where K, L and P are integers. $|K| + |L|$ is called the resonance order. Its value 1, 2, 3 … is respectively driven by a dipolar, quadripolar and sextupolar component of the field. P is the symmetry of the driving term. For example in cyclotrons, the third order coupling $\nu_r = 2\nu_z$, called , the Walkinshaw resonance is frequently encountered and considered as one of the most destructive.

As shown in (24), (26) and (27) the betatron oscillation derives from the field index and their evolution from the injection to the extraction can be calculated. As $\nu_{r,z}(r) \approx \nu_{r,z}(\gamma)$, one can plot the tunes as a function of the beam energy. Figure 22 shows that those critical diagram region can be rapidly crossed during the acceleration process, Therefore not damaging the beam.

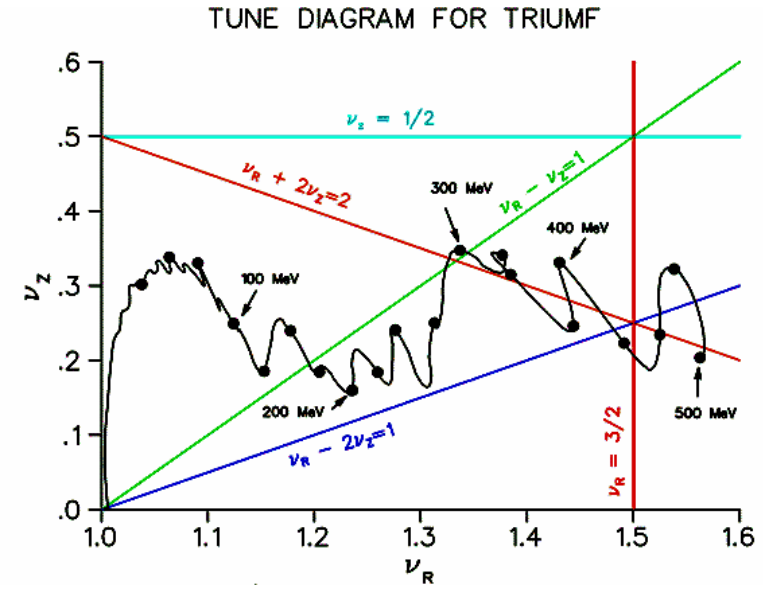

Fig. 22: Tune diagram from TRIUMF

The minimum number of sectors or symmetry periods in a cyclotron is fixed by the fundamental resonance $\nu_r = N/2$. At the cyclotron injection, $\nu_r \approx \gamma = 1$ and if $N = 2$, the cyclotron will be unstable from the centre. Therefore such a cyclotron does not exist.

From the same fundamental resonance, the increase of the sector number to 3 or 4 gives a limit $\nu_r \approx \gamma = 3/2$ or $4/2$ which for proton represent 470 MeV and 938 MeV. Hence, higher energies will require more sectors.

9 Cyclotron as a separator

The cyclotron can have two functions: acceleration and selection. The equations (9) and (12) imply that for an ion with a given q_0/m_0 ratio, acceleration is only possible for a given RF frequency and field level. This isochronous ion will be fully accelerated to the extraction.

An ion with a different q/m ratio will not have the right revolution frequency. The beam will not be isochronous. A phase shift of this ion compared to the RF phase during acceleration appears, giving a lack of acceleration. When the phase φ reaches 90°, the beam is decelerated and lost.

The phase shift definition is:

$$\Delta\varphi = 2\pi N h \frac{1}{\gamma^2} \frac{\Delta(m/Q)}{m_0/Q_0}$$

The figure below shows one isochronous beam ($^{36}Ar^{6+}$) and another beam ($^{18}O^{3+}$) whose mass over charge ratio differs by a few 10^{-4} [8]. In the cyclotron CIME, the non-isochronous beam is lost around a radius of 800 mm.

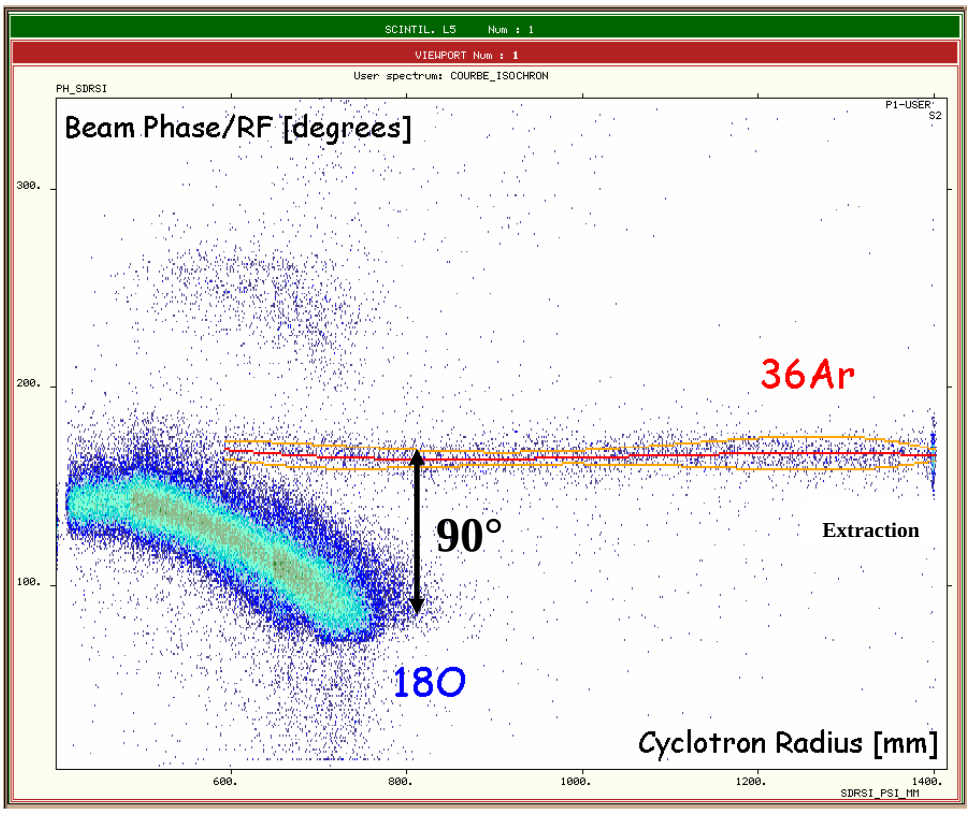

The mass resolution is by definition

$$R = \frac{\Delta\left(\frac{m}{q}\right)}{\frac{m_0}{q_0}} = \frac{1}{2\,\pi\; h\, N_{\text{turn}}}$$

We want R as small as possible in order to have as high a selectivity of the cyclotron as possible. Then for a given RF harmonic h, the number of turn N_{turn} needs to be as large as possible. This is obtained by lowering the accelerating voltage, thus getting a smaller turn separation but inducing a poor injection and/ or extraction efficiencies.

CIME example:

$h = 6$, $N_{\text{turn}} = 280$ ⇨ $R = 10^{-4}$, meaning that ions with a $m/q > 1.0001 \times m_0/q_0$ will not be extracted This is one of the great challenges for new exotic beam machines with isobars as close as 10^{-5}. Other means must be found to separate those ions.

10 Working diagram

An easy way to represent and visualize the capability of a cyclotron is to put together the field, frequency and the voltage of the source limitation on a same diagram, each quantity being linked for a given ion by the q/m ratio. One remarks the interest of trying to make use of the harmonic of the RF frequency. The energy range is largely increased. The mean field B_{cime} is strictly limited in the high field level because of the coil constraints but the lower limit can be pushed down if necessary. Finally, the source voltage will also be a limiting factor because the magnetic rigidity required to inject in the cyclotron depends on it : $B\rho = \sqrt{2Am_{\text{u}}V_{\text{source}}/q}$. In this diagram, the beams of identical q/m ratio are placed on a straight line.

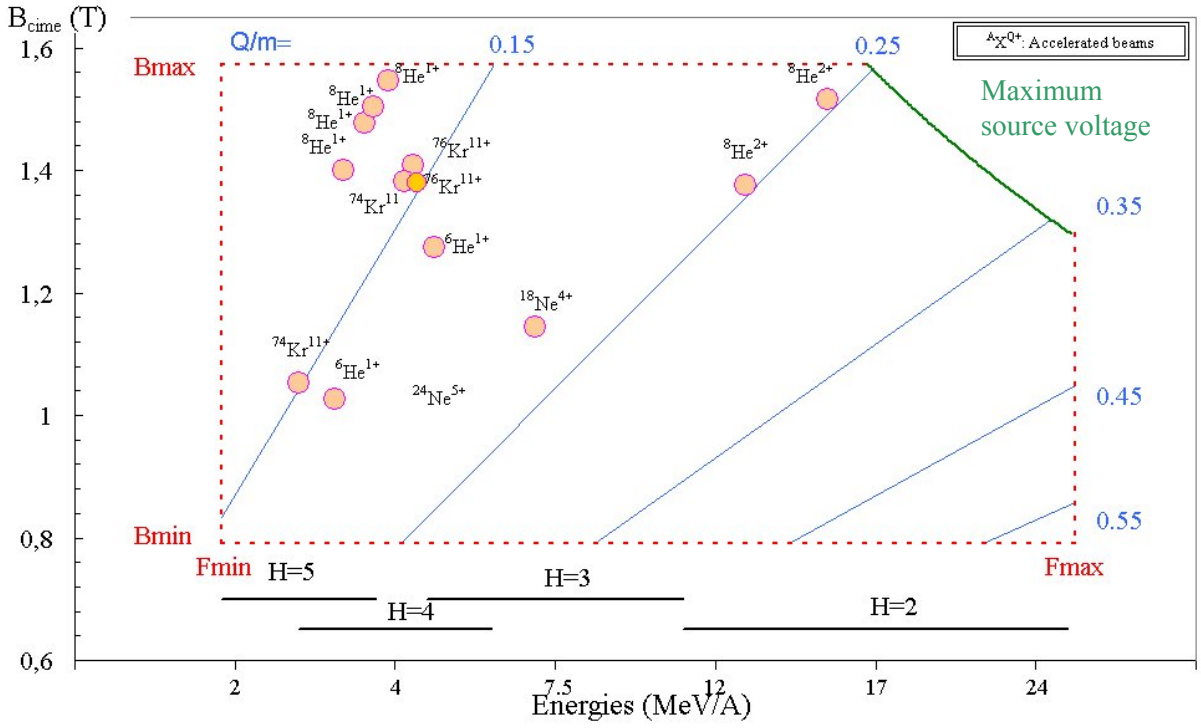

Acknowledgements

I would like to thank E. Baron for many instructive discussions and to share with me his educational skill. B. Launé (Orsay, France) who supplied me with much information on superconducting cyclotron behaviour.

References

[1] E. O. Lawrence and M.S. Livingston, Phys. Rev. 40 (1932) 19

[2] L. H. Thomas, Phys. Rev. 54 (1938) 580

[3] Proceedings of the international conference on sector-focused cyclotron. University of California, Los Angeles, 1962 , North–Holland publishing company 1962

[4] H. Blosser and D. Johnson, Focusing properties of superconducting cyclotrons, NIM 121 (1974) 301-306

[5] M. Lieuvin, Commissioning of SPIRAL, 6th European Particle Accelerator Conference : EPAC '98 Stockholm, Sweden ; 22 - 26 Jun 1998

[6] P. Bertrand, LIONS: a new of Fortran 90 codes for the SPIRAL project at GANIL, 4th International Conference on Charged-particle Optics : CP-4 Tsukuba, Japan ; 3 - 6 Oct 1994 . Publ. in: Proceedings K Ura, M Hibino, Komuro, M Kurashige, S Kurokawa et al Nucl. Instrum. Methods Phys. Res., A : 363 (1995) 1-2 (211-214).

[7] M. Duval, M, Bourgarel, M P , Ripouteau, New compact cyclotron design for SPIRAL, 14th International Conference on Magnet Technology - MT-14 Tampere, Finland ; 11 - 16 Jun 1995 . Publ. in: Proceedings IEEE Trans. Magn., 1996 APS (2194-2196).

[8] B. Launé et al., The diagnostic system for SPIRAL R.I.B. Facility, 14th Int. Cyclotron conf. Capetown, 1995

Bibliography

Textbooks

S. Humphries, jr., J. Wiley & Sons 1986, Principles of Charged Particle Acceleration.

H. Bruck, Bibl. des Scienc. et Tech. Nucléaires 1966, Accélérateurs Circulaires de Particules.

J. J. Livingood, D. van Nostrand Comp. 1961, Principles of Cyclic Particle Accelerators.

Conference Proceedings

Proceedings of the International Conferences on Sector-focused Cyclotrons and on Cyclotrons and their application:

ICC1, Informal Conference on sector-focused Cyclotrons 1959 in Sea Island, NAS-NRC, Publ.656 (1959)

ICC2, Int. Conference 1962 in Los Angeles, Nucl. Inst.& Meth. 18, 19 (1962)

ICC3, Int. Conference 1963 in Geneva, CERN 63-19 (1963)

ICC4, Int. Conference 1966 in Gatlinburg, IEEE Trans. NS-13(4) (1966)

ICC5, 5th Int. Cyclotron Conference 1969 in Oxford, McIllroy, Butterworth (1971)

ICC6, 6th Int. Cyclotron Conference 1972 in Vancouver, AIP Conf. Proc. N°9 (1972)

ICC7, 7th Int. Cyclotron Conference 1975 in Zürich, Birkhäuser (1975)

ICC8, 8th Int. Cyclotron Conference 1978 in Bloomington, IEEE Trans. NS-26(2) (1979)

ICC9, 9th Int. Cyclotron Conference 1981 in Caen, les Editions de Physique (1982)

ICC10, 10th Int. Cyclotron Conference 1984 in East Lansing, IEEE, New York (1984)

ICC11, 11th Int. Cyclotron Conference 1986 in Tokyo, Ionics Publishing Tokyo (1987)

ICC12, 12th Int. Cyclotron Conference 1989 in Berlin, World Scientific Publ. (1991)

ICC13, 13th Int. Cyclotron Conference 1992 in Vancouver, World Scientific Publ. (1993)
ICC14, 14th Int. Cyclotron Conference 1995 in Cape Town, World Scientific Publ Co. (1996)
ICC15, 15th Int. Cyclotron Conference 1998 in Caen, Institute of Physics Publ. (1999)
ICC16, 16th Int. Cyclotron Conference 2001 in East Lansing, American Inst. of Ph., New York (2001)

Contribution to CERN Accelerator Schools

W. Joho, CAS Aarhus 1986, CERN 87-10 (1987) 1 "Modern Trends in Cyclotrons"
H.L. Hagedoorn et al., CAS Jülich 1990, CERN 91-04 (1991) 323 "Introduction to Cyclotron"
H.L. Hagedoorn et al., CAS Leewenhorst 1991, CERN 92-01 (1992) 1 "Hamilton Theory"
P. Heikinnen, CAS Jyväskylä 1992, CERN 94-01 (1994) "Cyclotrons" and "Injection and Extraction"
T. Stammbach, CAS La Hulpe, 1994, CERN 96-02 (1996) "Introduction to Cyclotrons"